

Multivariate Prototype Representation for Domain-Generalized Incremental Learning

Can Peng^a, Piotr Koniusz^{a,c,**}, Kaiyu Guo^b, Brian C. Lovell^b, Peyman Moghadam^{a,d}

^aData61, CSIRO, Brisbane, Queensland, Australia

^bThe University of Queensland, Brisbane, Queensland, Australia

^cThe Australian National University, Canberra, Australia

^dQueensland University of Technology, Brisbane, Queensland, Australia

ABSTRACT

Deep learning models suffer from catastrophic forgetting when being fine-tuned with samples of new classes. This issue becomes even more pronounced when faced with the domain shift between training and testing data. In this paper, we study the critical and less explored Domain-Generalized Class-Incremental Learning (DGCIL). We design a DGCIL approach that remembers old classes, adapts to new classes, and can classify reliably objects from unseen domains. Specifically, our loss formulation maintains classification boundaries and suppresses the domain-specific information of each class. With no old exemplars stored, we use knowledge distillation and estimate old class prototype drift as incremental training advances. Our prototype representations are based on multivariate Normal distributions whose means and covariances are constantly adapted to changing model features to represent old classes well by adapting to the feature space drift. For old classes, we sample pseudo-features from the adapted Normal distributions with the help of Cholesky decomposition. In contrast to previous pseudo-feature sampling strategies that rely solely on average mean prototypes, our method excels at capturing varying semantic information. Experiments on several benchmarks validate our claims.

arXiv:2309.13563v1 [cs.CV] 24 Sep 2023

1 Introduction

Despite the progress in deep learning, many algorithms fail when the data distribution changes. Objects of interest from new classes can continually appear, and simultaneously the old class data might be inaccessible due to data storage limitations, privacy, or licensing issues. Under such conditions, direct fine-tuning of deep learning models with the new class data will make a deep learning model lose the performance on previously-learned tasks – the catastrophic forgetting problem. Also, when trained models are deployed into new data domains stemming from diverse sources of data, the model often fails to generalize to out-of-distribution cases. Incremental Learning (IL) addresses the problem of catastrophic forgetting posed by the incoming data whose distribution changes over time. Domain Generalization (DG) tackles the out-of-distribution problem caused by the distribution shift between training and testing data. Unfortunately, IL and DG are usually considered separate problems. Yet, for autonomous vehicles or robots, new classes of objects such as new road signs, new means of transport, and various surrounding buildings can continually appear and need to be learnt without forgetting the already-learned visual concepts. The system also has to perform well under conditions that differ from the training domain, including variations in lighting, weather, infrastructure designs, *etc.* Domain-Generalized Class-Incremental Learning (DGCIL) addresses these two scenarios that require simultaneous handling

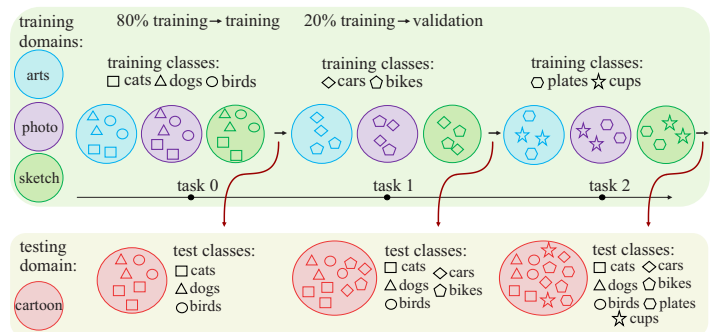


Fig. 1: Domain-Generalized Class-Incremental Learning. Samples of new classes are provided from a fixed set of training domains for each incremental learning step t . During testing, the model has to perform well on all the categories learnt so far under an unseen testing domain. Each domain becomes a testing domain once, *i.e.*, four separate runs are needed, over which average accuracy is calculated.

of catastrophic forgetting and out-of-distribution recognition. DGCIL approaches have to achieve good performance under novel test domains and a significant intake of new visual categories.

Figure 1 illustrates the DGCIL paradigm. During training, for each incremental step, with only new class data available, the model needs to learn representations of new classes as well as maintain representations of old classes. At the inference stage, the model is required to perform well in all the classes learnt so far on novel domains (not seen in training). Compared with IL and DG, DGCIL is more challenging and less explored.

**Corresponding author.

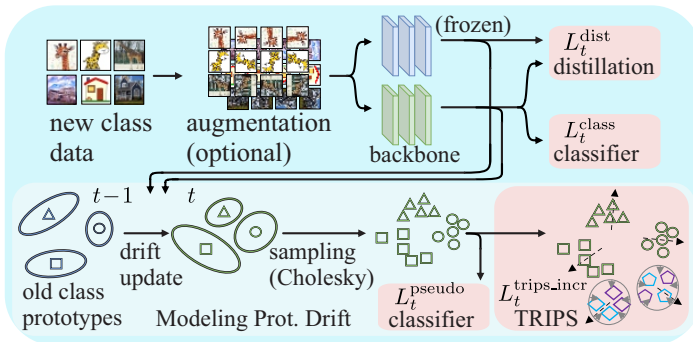


Fig. 2: The TRIPS pipeline. During the incremental step t , we pass new class samples through the old (frozen) and the current models. A classifier loss L_t^{class} and a distillation loss L_t^{dist} are applied. The mean and covariance matrices of each class prototype are updated due to the feature drift between models. Subsequently, pseudo-samples are obtained from covariances and passed to pseudo-classifier L_t^{pseudo} . Finally, our TRIPS pushes feature vectors of different classes apart (black dashed arrows), while suppressing domain-specific information (grey arrows facing inwards).

While some efforts have been made to explore continual domain adaptation which evaluates the model on continually arriving classes and domains (Buzzega et al., 2020; Knights et al., 2022; Volpi et al., 2021; Xie et al., 2022; Liu et al., 2023), DGCIL simultaneously targets out-of-domain generalization. In contrast, the problem of continual domain adaptation focuses on adaptation under training domain shift. To the best of our knowledge, MSL_MOV (Simon et al., 2022) is the only work that targets a similar task. However, in their setting, old class exemplars from each training domain need to be stored which might cause data privacy or storage issues, *i.e.*, storing exemplars may be simply not an option. In contrast, in this work, we design an exemplar-free DGCIL model.

As we are interested in an exemplar-free setting, we remove the exemplars from the experimental setting. For a baseline, we modify the only existing DGCIL model, MSL_MOV, to work with the prototypes instead of exemplars.

Moreover, we notice that the evaluation protocol introduced by MSL_MOV is limited to their specific pipeline design, and may be biased towards old classes. Specifically, within each incremental step, MSL_MOV performs three-stage training (training for each domain progressively). For each incremental step, MSL_MOV reports the average results from three stages. The evaluation results within such a training procedure may be not universal as they are biased towards first- and early-stage results, *e.g.*, the first stage of a new incremental step may be biased towards good performance on old classes, whereas the last stage may be biased towards new classes. Also, the first stage may be more aligned with the test domain than the model from all three stages. Thus, averaging the results of three stages may make results on old classes look better compared to a one-off evaluation at the end of the incremental step.

Thus, we propose a more realistic evaluation protocol as follows. During each incremental step, we only perform a one-

time evaluation once the given incremental step learnt from all training domains (all stages are completed). Based on the publicly available domain generalization benchmark DomainBed (Gulrajani and Lopez-Paz, 2021), we build our framework and method. We reproduce MSL_MOV in our evaluation setting for fair comparisons with our approach. Figure 4 illustrates the difference in both evaluation settings.

As we adopt the challenging exemplar-free DGCIL setting, we propose *TRIPlet loss with Pseudo old-class feature Sampling* (TRIPS). Figure 2 illustrates our model. During training, we adopt a novel variant of triplet loss that focuses on distinguishing semantic information while suppressing the domain information. The goal of such a loss is to improve the generalization of the model towards an unseen test distribution. In addition, we apply knowledge distillation to maintain previously-learned knowledge and prevent catastrophic forgetting. Moreover, old classes are described by class prototype representations based on the multivariate Normal distributions. As incremental sessions progress, the drift associated with each mean and covariance matrix of each prototype is estimated, and prototype representations are updated accordingly before we sample old-class pseudo-features via the Cholesky decomposition. Such pseudo-features help preserve the knowledge of old classes from the past sessions and maintain the class separation by TRIPS, facilitating balanced performance on old and new class concepts.

Our main contributions are summarised as follows:

- i. With data storage, privacy, and licensing issues in mind, we propose an exemplar-free approach for DGCIL, based on *TRIPlet loss with Pseudo old-class feature Sampling*. The goal of TRIPS is to keep features of different classes apart while suppressing domain-related feature information, which facilitates domain generalization.
- ii. As TRIPS has to handle old and new classes incrementally, we introduce class-wise prototype representations based on the multivariate Normal distributions. We estimate their drift (for each mean/covariance) as the backbone is updated along incremental sessions. We then sample pseudo-features for old classes from such distributions.
- iii. Details of model selection (validation procedure), data splitting, and evaluation strategies are important for reproducibility. As exemplar-free DGCIL models do not exist, we provide a comprehensive DGCIL task setting for exemplar-free DGCIL including (i) validation procedure, (ii) evaluation setting reflecting the performance of each incremental step, and (iii) the overall and balanced performance based on the domain-wise and class-wise average and harmonic accuracy, respectively. The code with validation/evaluation protocols will be released.

2 Related Works

In this section, we explain related works in Incremental Learning (IL), Domain Generalization (DG), and Domain-Generalized Class-IL (DGCIL).

Incremental Learning Settings. IL requires the model to continually learn new tasks from a sequential data stream without forgetting the past. IL can be categorized into three sub-tasks: Task-IL, Class-IL, and General IL. The main difference between them is whether task boundaries are accessible during training and testing. Task-IL, the simplest IL scenario, allows access to task boundaries during both training and testing (Li and Hoiem, 2017). Different from Task-IL, the Class-IL scenario only provides task boundaries during training (Kirkpatrick et al., 2017; Chaudhry et al., 2018; Aljundi et al., 2018; Rebuffi et al., 2017; Hou et al., 2019). During testing, a Class-IL model is required to have a unified classifier that can classify all classes learnt so far. General IL, a newly emerged IL scenario, is a more practical setting than Task-IL and Class-IL. In this setting, the task boundaries are not accessible during either training or testing (Xie et al., 2022; Ji et al., 2022; Li et al., 2022). However, General-IL does not model out-of-distribution scenes to facilitate novel test distributions. Some General-IL methods consider domain adaptation (Buzzega et al., 2020; Xie et al., 2022) by incrementally adding new classes/domains and performing testing on classes/domains learnt so far. They do not consider unseen domains during testing. In contrast, we study Domain-Generalized IL to preserve old class knowledge, and continually learn new class concepts, while generalizing well to unseen test distributions.

Solutions to Incremental Learning. Current IL methods are often based on: regularization, dynamic architecture, or old exemplar replay. Advanced regularization terms impose constraints on the network update and mitigate catastrophic forgetting. Some models regularize the parameter updating according to their importance w.r.t. previously-learnt tasks (Kirkpatrick et al., 2017; Chaudhry et al., 2018; Aljundi et al., 2018). Other models maintain past feature distribution by knowledge distillation on logits (Li and Hoiem, 2017; Rebuffi et al., 2017; Hou et al., 2019) or on intermediate features (Simon et al., 2021; Roy et al., 2023). Dynamic architecture (Yoon et al., 2018; Douillard et al., 2022) assigns each new task with a task-specific sub-network to balance the stability and plasticity trade-off. Old exemplar replay retains some old class samples for experience replay during new task training to refresh the model memory (Rebuffi et al., 2017; Hou et al., 2019; Xie et al., 2022; Li et al., 2022; Ji et al., 2022).

Domain Generalization. DG approaches are required to make good predictions on novel test domains. Many DG models reduce domain gaps in the latent space and obtain easy-to-transfer model parameters by meta-learning (Dou et al., 2019), data augmentation (Zhang et al., 2018; Zhou et al., 2021), or capturing causal relations (Arjovsky et al., 2019; Krueger et al., 2021). Although a myriad of domain generalization algorithms has been proposed, they use various experimental settings, such as different datasets and model selection criteria (Gulrajani and Lopez-Paz, 2021). Gulrajani and Lopez-Paz (2021) propose a benchmark testbed called DomainBed and argue that when equipped with modern neural network architectures and data augmentation techniques, empirical risk minimization (ERM) achieves state-of-the-art performance.

Domain-Generalized Class-IL (DGCIL). In this paper, we

study Domain-Generalized Class-Incremental Learning, bridging the gap between the Class-IL (CIL) and DG problems. DGCIL solves both catastrophic forgetting due to the semantic shift and domain generalization beyond training domains. Compared with CIL and DG, DGCIL is more challenging and less explored. MSL_MOV (Simon et al., 2022) is the only related work that explores a similar problem by the use of Mahalanobis metrics for classification in unseen domains. MSL_MOV also uses old class exemplars and exponential moving average knowledge distillation to overcome catastrophic forgetting. However, in many situations, old class exemplars should not be used (privacy, storage, *etc.*) and the number of parameters of MSL_MOV grows linearly. In this paper, we provide a comprehensive task setting for DGCIL and propose an exemplar-free DGCIL method.

3 What is the DGCIL About?

A DGCIL model (similar to CIL) learns new tasks continually in several steps but the model is required to perform well on unseen test domains (domain-invariant model). The DGCIL algorithms have two goals: (i) learning new class concepts while maintaining knowledge of old class concepts, and (ii) learning semantic invariance from training data with domain-specific information. The latter property helps the model generalize to out-of-distribution cases during testing. Figure 1 describes the training and testing of DGCIL.

Specifically, a DGCIL task has $T + 1$ steps each associated with a sub-task \mathcal{T}_t where $t \in \{0, 1, \dots, T\}$. Let \mathcal{T}_0 denote the base task and $\{\mathcal{T}_t : t \geq 1\}$ be incremental tasks. The t -th task has to learn $|C_t|$ new class concepts with training samples of categories from set C_t . Considering the possible memory limitation in realistic conditions, we opt for an exemplar-free setting. Training data from different tasks has no overlap in class labels or samples, thus $C_t \cap C_{t'} = \emptyset$ if $t \neq t'$. During each incremental learning task, training samples from Z different domain distributions are provided by sets \mathcal{D}_z where $z \in \{1, \dots, Z\}$. The total training data is represented as $\mathcal{D}_{\text{train}} = \mathcal{D}_1 \cup \mathcal{D}_2 \dots \cup \mathcal{D}_Z$. During testing, the model will be evaluated on all classes learnt up to t in an unseen domain $\mathcal{D}_{\text{test}} = \mathcal{D}_{Z+1}$. Thus, $C_{\text{train}} = C_t$ and $C_{\text{test}} = C_0 \cup C_1 \dots \cup C_t$, while domains $\mathcal{Z}_{\text{train}} \cap \mathcal{Z}_{\text{test}} = \emptyset$.

4 Proposed Approach

In this section, we outline our algorithm, which consists of: (i) triplet loss which teaches the model to distinguish semantic information across different classes while suppressing domain-specific information, (ii) cross-entropy knowledge distillation which prevents catastrophic forgetting of past knowledge, (iii) prototype representations based on the multivariate Normal distribution with a drift mechanism that adapts prototypes from previous sessions to the feature space of the current session, and (iv) sampling mechanism via Cholesky decomposition.

4.1 Learning New Classes

Our approach consists of three components: (i) learning new knowledge, (ii) preserving the former knowledge, and (iii) handling out-of-distribution cases.

For the first component, we adopt the commonly used strategy based on the cross-entropy loss using the ground truth labels and softmax-normalized model output over all classes learnt so far. Let a set of sample-label pairs (\mathbf{x}, y) for the current session t be stored in batch \mathcal{B} . Let the set of classes observed so far for the session/step t where $t \leq T$ be denoted as $C' = C_0 \cup C_1 \dots \cup C_t$. Then we have the new knowledge learning for the step t :

$$L_t^{\text{class}} = -\frac{1}{|\mathcal{B}|} \sum_{(\mathbf{x}, y) \in \mathcal{B}} \log \left(\frac{\exp(\boldsymbol{\theta}_{ty}^\top f_t(\mathbf{x}))}{\sum_{c \in C'} \exp(\boldsymbol{\theta}_{tc}^\top f_t(\mathbf{x}))} \right). \quad (1)$$

Notice that while \mathcal{B} only contains samples of classes in set C_t , the denominator of Eq. (1) runs over all classes observed in sessions/steps $0, \dots, t$. Function $f_t(\cdot)$ denotes our feature extractor trained in session t . Parameters of $f_t(\cdot)$ are initialized by coping from parameters of $f_{t-1}(\cdot)$. Moreover, $\boldsymbol{\theta}_{ty}$ denotes a linear projection from session t for class $y \in C'$ (which is essentially an FC layer). Linear projection parameters $\boldsymbol{\theta}_{ty'}$ for $y' \in C''$ where $C'' = C' \setminus C_t$ are initialized by coping from $\boldsymbol{\theta}_{t'y'}$ where $t' = t - 1$. In practice, we also use bias terms b_{ty} , *i.e.*, we have a linear projection $\boldsymbol{\theta}_{ty}^\top f_t(\mathbf{x}) + b_{ty}$ but we skip b_{ty} for brevity.

4.2 Knowledge Distillation

As DGCIL approaches have to retain the knowledge from previous sessions and overcome catastrophic forgetting (Hinton et al., 2015), for our model we adopt simple knowledge distillation¹ to transfer responses of feature extractor $f_{t-1}(\cdot)$ to $f_t(\cdot)$ and linear projection $\boldsymbol{\theta}_{t-1}$ to $\boldsymbol{\theta}_t$ by cross-entropy. The samples of new classes are passed via frozen $f_{t-1}(\cdot)$ and $\boldsymbol{\theta}_{t-1}$ to distill through the lens of old classes from set $C'' = C_0 \cup C_1 \dots \cup C_{t-1}$ representing past sessions $t = 0, \dots, t - 1$ into $f_t(\cdot)$ and $\boldsymbol{\theta}_t$. We define distillation for the step t as:

$$L_t^{\text{dist}} = -\frac{1}{|\mathcal{B}|} \sum_{\mathbf{x} \in \mathcal{B}} \sum_{c \in C''} \pi_c^{t-1}(\mathbf{x}) \log(\pi_c^t(\mathbf{x})) \quad (2)$$

$$\text{where } \pi_c^t(\mathbf{x}) = \frac{\exp(\boldsymbol{\theta}_{tc}^\top f_t(\mathbf{x}))}{\sum_{c' \in C''} \exp(\boldsymbol{\theta}_{tc'}^\top f_t(\mathbf{x}))}. \quad (3)$$

In Eq. (2) and (3), π^t and π^{t-1} are the probability outputs of the current model (t) and the previous model ($t - 1$) when passing samples of current session t , denoted as $(\mathbf{x}, y) \in \mathcal{B}$, but distilling them through the lens of classes from the past sessions (set C''). Although batch \mathcal{B} contains pairs (\mathbf{x}, y) , we simply enumerate over data samples and so we slightly abuse our notation by writing $\mathbf{x} \in \mathcal{B}$. We also use the bias terms but we skip them in equations for clarity.

4.3 The TRIPS Loss

As DGCIL approaches have to perform well during testing on an unseen domain (out-of-distribution conditions), during

training, we want our model to capture the semantic information while suppressing the domain-specific information. To this end, we adapt our TRIPS formulation based on the triplet loss².

Specifically, we regard encoded feature vectors $f_t(\mathbf{x})$ and $f_t(\mathbf{x}')$ of samples \mathbf{x} and \mathbf{x}' with the same class labels $y(\mathbf{x}) = y(\mathbf{x}')$ but different domain labels $z(\mathbf{x}) \neq z(\mathbf{x}')$ as positive pairs, denoted as $\gamma_{\mathbf{x}, \mathbf{x}'}^+$. Moreover, we regard feature vectors $f_t(\mathbf{x})$ and $f_t(\mathbf{x}')$ with two different class labels $y(\mathbf{x}) \neq y(\mathbf{x}')$ but the same domain labels $z(\mathbf{x}) = z(\mathbf{x}')$ as negative pairs, denoted as $\gamma_{\mathbf{x}, \mathbf{x}'}^-$. To help the model learn to classify class concepts instead of domain concepts, the distance between positive pairs should be smaller than the distance between negative pairs. We employ the squared Euclidean distance $d(\mathbf{x}, \mathbf{x}') = \|f_t(\mathbf{x}) - f_t(\mathbf{x}')\|_2^2$ to measure the pairwise distance. Formally, positive and negative feature pairs are defined as:

$$\gamma_{\mathbf{x}, \mathbf{x}'}^+ = \begin{cases} 1 & \text{if } y(\mathbf{x}) = y(\mathbf{x}') \wedge z(\mathbf{x}) \neq z(\mathbf{x}'), \\ 0 & \text{otherwise,} \end{cases} \quad (4)$$

$$\delta_{\mathbf{x}, \mathbf{x}'}^- = \begin{cases} 1 & \text{if } y(\mathbf{x}) \neq y(\mathbf{x}') \wedge z(\mathbf{x}) = z(\mathbf{x}'), \\ 0 & \text{otherwise.} \end{cases} \quad (5)$$

Subsequently, we define our TRIPS loss as follows:

$$L_t^{\text{trips.base}} = \frac{1}{|\mathcal{B}|} \sum_{\mathbf{x} \in \mathcal{B}} \left[\max_{\mathbf{x}' \in \mathcal{B} \setminus \{\mathbf{x}\}} \gamma_{\mathbf{x}, \mathbf{x}'}^+ \cdot d(\mathbf{x}, \mathbf{x}') - \min_{\mathbf{x}'' \in \mathcal{B} \setminus \{\mathbf{x}\}} \gamma_{\mathbf{x}, \mathbf{x}''}^- \cdot d(\mathbf{x}, \mathbf{x}'') + m \right]_+, \quad (6)$$

where $[\phi]_+ \equiv \max(\phi, 0)$ is a ReLU to realize the triplet loss with margin m (set to 0 in our experiments). Although batch \mathcal{B} contains pairs (\mathbf{x}, y) , we enumerate only over data samples—we slightly abuse our notation by writing $\mathbf{x} \in \mathcal{B}$.

4.4 Modeling Prototype Drift

With no access to old data, we utilize old-class prototype representations to prevent catastrophic forgetting. Related works on incremental learning tasks commonly use the per-class mean-based prototype (Yu et al., 2020; Zhu et al., 2021b). However, these prototypes are insufficient for capturing intra-class variance resulting from multiple samples from different training domains as they only capture first-order statistics of class-wise feature distribution. In our approach, we utilize both the mean vector and covariance matrix for each class to enhance the representation of distribution of each old class. By incorporating covariance around its mean, the multivariate Normal distribution offers a more accurate model of class-specific boundaries. Furthermore, compared to isotropic/univariate Normal distributions or mean vectors (first-order statistics), considering second-order statistics through multivariate Normal distributions provides a more realistic distribution model. Figure 3 illustrates the latent feature space with class-wise distributions.

¹Kindly note we do not claim the methodology of Sections 4.1 and 4.2 *per se* as contributions. These are prerequisites required in our model.

²Kindly note we do not claim standard triplet loss as our contribution. Our contribution is in the bespoke design that separates classes while discarding domain-specific information.

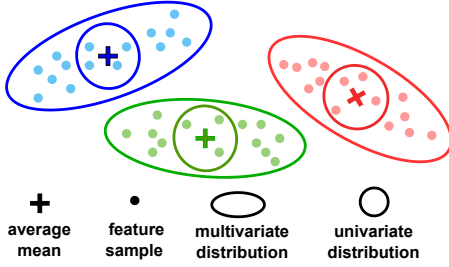


Fig. 3: An example of the latent space and class-wise feature distributions. Due to the intra-class variance (multiple samples from several training domains), the single per-class feature mean (which is the first-order statistic) is not sufficient to represent the class distribution well. The old class distribution can be better captured by the mean and covariance matrix (the multivariate Normal distribution). The multivariate Normal distributions (second-order statistics) capture class boundaries better than isotropic/univariate Normal distributions and first-order statistics such as the mean vectors.

Given our prototype representations are modeled as the multivariate Normal distribution per class, we can draw pseudo-samples from these distributions for old classes. However, as the feature extractor changes over time, we need to account for the prototype drift in the evolving feature space. As the new classes are being learnt, the model is updated, and the feature distribution changes. Consequently, we cannot simply use the previously stored prototype representations for old classes without accounting for this drift.

With no access to old class exemplars, we capture the drift of features through the lens of samples of new classes passed through the current and past feature extractor, $f_t(\cdot)$ and $f_{t-1}(\cdot)$, respectively. Essentially, $f_t(\mathbf{x}) - f_{t-1}(\mathbf{x})$ captures the changes. Such a modeling approach assumes that the semantics of old tasks and new tasks must somewhat overlap, *i.e.*, the past feature space and current feature spaces are not completely disjoint semantically. We define:

$$\Delta\phi(\mathbf{x}) = f_t(\mathbf{x}) - f_{t-1}(\mathbf{x}), \quad (7)$$

$$w(\mathbf{x}, \boldsymbol{\mu}) = \exp\left(-\frac{1}{2\sigma^2}\|f_{t-1}(\mathbf{x}) - \boldsymbol{\mu}\|_2^2\right), \quad (8)$$

where $\Delta\phi(\mathbf{x})$ is the drift for an individual sample \mathbf{x} , and $w(\mathbf{x}, \boldsymbol{\mu}^{t-1})$ captures similarity of \mathbf{x} w.r.t. prototype mean $\boldsymbol{\mu}^{t-1}$ from step $t-1$ given some bandwidth hyper-parameter $\sigma > 0$ (set to 0.5 in all our experiments). Let the drift of prototype mean be defined as:

$$\Delta\boldsymbol{\mu}_c = \frac{\sum_{\mathbf{x} \in \mathcal{B}} w(\mathbf{x}, \boldsymbol{\mu}_c^{t-1}) \cdot \Delta\phi(\mathbf{x})}{\sum_{\mathbf{x}' \in \mathcal{B}} w(\mathbf{x}', \boldsymbol{\mu}_c^{t-1})}, \quad (9)$$

$$\Delta\boldsymbol{\mu}_c^b = \eta\Delta\boldsymbol{\mu}_c^{b-1} + (1-\eta)\Delta\boldsymbol{\mu}_c. \quad (10)$$

We go over batches \mathcal{B}_b where $b = 1, \dots, B$ but we drop subscript b from \mathcal{B}_b for brevity. The final expression after B batches is:

$$\boldsymbol{\mu}_c^t = \boldsymbol{\mu}_c^{t-1} + \Delta\boldsymbol{\mu}_c^B. \quad (11)$$

Hyper-parameter η (set to 0.1 in all our experiments) controls the so-called exponential moving average.

Next, we estimate covariance drift $\boldsymbol{\Sigma}'_c$ for batches \mathcal{B}_b , $b = 1, \dots, B$. We drop subscript b from \mathcal{B}_b for brevity. As $\boldsymbol{\Sigma}'_c$ is estimated from a limited number of samples, we apply to it the shrinkage operator (Ledoit and Wolf, 2004) known to estimate covariance matrices reliably in such circumstances. We apply the exponential moving average to obtain $\boldsymbol{\Sigma}'_c^b$:

$$\boldsymbol{\Sigma}'_c = \frac{\sum_{\mathbf{x} \in \mathcal{B}} w(\mathbf{x}, \boldsymbol{\mu}_c^{t-1}) \cdot (f_t(\mathbf{x}) - \boldsymbol{\mu}_c^t)(f_t(\mathbf{x}) - \boldsymbol{\mu}_c^t)^\top}{\sum_{\mathbf{x}' \in \mathcal{B}} w(\mathbf{x}', \boldsymbol{\mu}_c^{t-1})}, \quad (12)$$

$$\boldsymbol{\Sigma}'_c^b = \eta\boldsymbol{\Sigma}'_c^{b-1} + (1-\eta)((1-\alpha)\boldsymbol{\Sigma}'_c + \alpha\mathbb{I}). \quad (13)$$

which leads to the final expression $\boldsymbol{\Sigma}'_c = \boldsymbol{\Sigma}'_c^B$ after B batches. Hyper-parameter η controls the exponential moving average (set to 0.1 in all our experiments). Moreover, $0 \leq \alpha \leq 1$ decides by how much covariance is shrunk towards the isotropic Normal distribution (set to 0.05 in all our experiments).

We then sample pseudo-features of past classes from our prototype representations during processing each mini-batch \mathcal{B} .

$$\boldsymbol{\phi}'_c \sim \mathcal{N}(\boldsymbol{\mu}'_c, \boldsymbol{\Sigma}'_c) \quad \text{where } c \sim \mathcal{U}(1, |C''|), \quad (14)$$

where $\mathcal{N}(\boldsymbol{\mu}'_c, \boldsymbol{\Sigma}'_c)$ denotes the multivariate Normal distribution with mean $\boldsymbol{\mu}'_c$ and covariance $\boldsymbol{\Sigma}'_c$, and $\mathcal{U}(1, |C''|)$ denotes the uniform distribution having $1/|C''|$ probability within support region $[1, |C''|]$ (and zero elsewhere), and C'' defined in Section 4.2 is set of classes from sessions $0, \dots, t-1$. Finally, we note that:

$$\boldsymbol{\phi}'_c \sim \mathcal{N}(\boldsymbol{\mu}'_c, \boldsymbol{\Sigma}'_c) \iff \boldsymbol{\phi}'_c = \boldsymbol{\mu}'_c + \text{Chol}(\boldsymbol{\Sigma}'_c)\mathbf{v} \quad \text{where } \mathbf{v} \sim \mathcal{N}(\mathbf{0}, \mathbb{I}), \quad (15)$$

where $\text{Chol}(\cdot)$ is the Cholesky decomposition³ of the symmetric positive definite matrix.

4.5 Integration of Class Learning and the TRIPS Loss

To further preserve old class information and balance the extreme data imbalance (exemplar-free approach), during the new sessions, we want to ensure the classifier and TRIPS model have access to pseudo-samples obtained by Eq. (15) in order to update classifier parameters, keep features of different classes separated (not only new class features but also old class features despite the lack of access to old class samples) while actively suppressing the domain-wise information. Thus, the classification loss in Eq. (1) is merged at the final stage with the classification loss on pseudo-features in Eq. (16).

Let $(\boldsymbol{\phi}, y) \in \mathcal{S}$ be pseudo-samples (with labels $y \in C''$) obtained by Eq. (15) for session t and batch \mathcal{B} . We define:

$$L_t^{\text{pseudo}} = -\frac{1}{|\mathcal{S}|} \sum_{(\boldsymbol{\phi}, y) \in \mathcal{S}} \log\left(\frac{\exp(\boldsymbol{\theta}_{ty}^\top \boldsymbol{\phi})}{\sum_{c \in C'} \exp(\boldsymbol{\theta}_{tc}^\top \boldsymbol{\phi})}\right). \quad (16)$$

³Cholesky decomposition has a fast implementation in PyTorch and stable numerical results compared to the SVD-based matrix square root.

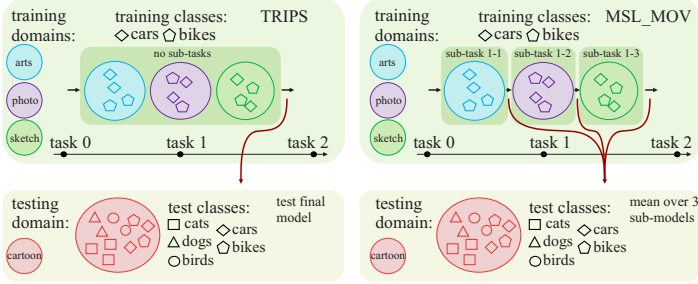


Fig. 4: Evaluation protocols for DGCIL. (right) The only existing protocol, implemented by MSL_MOV, evaluates each incremental step by averaging performance on individual sub-tasks. As the first sub-task may be biased towards old classes from the previous incremental step, we argue that a better evaluation protocol should avoid sub-tasks. Also, the first sub-task may be more aligned with the test domain than the whole task, so evaluation should take place at the end of task instead. (left) TRIPS performs incremental training step without splitting the problem into sub-tasks. We evaluate the samples from the test domain once the incremental step finishes. We adopt this evaluation protocol on TRIPS and MSL_MOV.

Subsequently, the TRIPS in Eq. (6) is redefined as Eq. (17):

$$L_t^{\text{trips.incr}} = \frac{1}{|\mathcal{B}|} \sum_{\mathbf{x} \in \mathcal{B}} \left[\max_{\mathbf{x}' \in \mathcal{B} \setminus \{\mathbf{x}\}} \gamma_{\mathbf{x}, \mathbf{x}'}^+ \cdot d(\mathbf{x}, \mathbf{x}') - \min \left(\min_{\mathbf{x}'' \in \mathcal{B} \setminus \{\mathbf{x}\}} \gamma_{\mathbf{x}, \mathbf{x}''}^- \cdot d(\mathbf{x}, \mathbf{x}''), \min_{\phi \in \mathcal{S}} \|f_t(\mathbf{x}) - \phi\|_2^2 \right) + m \right]. \quad (17)$$

Notice that negative-pair labels γ^- between $\mathbf{x} \in \mathcal{B}$ and pseudo-samples $\phi \in \mathcal{S}$ always equal 1. Pseudo-samples are domain agnostic by design, and pseudo-sample set \mathcal{S} and batch set \mathcal{B} have class set $\mathcal{C}'' \cap \mathcal{C}_t = \emptyset$. Also, to balance the old and new class performance, we sample the same number of pseudo-features as new class features $|\mathcal{S}| = |\mathcal{B}|$.

The full loss. L_t for step $t \geq 0$ and hyper-parameters λ & λ' is:

$$L_t = \begin{cases} L_0^{\text{class}} + \lambda L_0^{\text{trips.base}}, & \text{if } t = 0, \\ L_t^{\text{class}} + L_t^{\text{pseudo}} + \lambda L_t^{\text{trips.incr}} + \lambda' L_t^{\text{dist}} & \text{if } t \geq 1, \end{cases} \quad (18)$$

where λ and λ' are hyper-parameters that balance different loss terms. By diagnosing the loss value for each loss term, we set $\lambda = 1$ and λ' to 30 for all our experiments to ensure that all loss terms contribute similar level of penalty.

5 Experiments

In this section, we compare our proposed method with existing approaches in both incremental learning and domain generalization. We start by introducing the experimental details.

Datasets. Three domain generalization benchmark datasets PACS (Li et al., 2017), OfficeHome (Venkateswara et al., 2017), and DomainNet (Saito et al., 2019) are used for our experiments. PACS (Li et al., 2017) contains 7 classes from 4 domains: Art, Cartoon, Photo, and Sketch. It provides challenging recognition scenarios with significant shifting between different

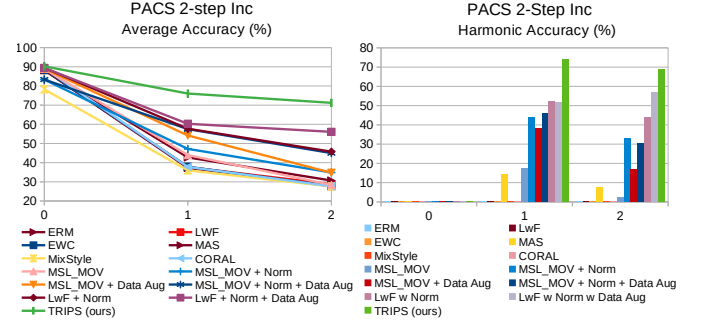


Fig. 5: Domain-average performance of each incremental step under the 2-step incremental setting on the PACS dataset.

domains. OfficeHome (Venkateswara et al., 2017) is a large-scale dataset that contains 65 classes from 4 domains: Real, Clipart, Art, and Product. DomainNet (Saito et al., 2019) is also a large-scale dataset that contains 126 classes from 4 domains: Real, Clipart, Painting, and Sketch. To comprehensively evaluate the performance of our proposed method, we perform various multi-step incremental learning scenarios on these datasets. Specifically, according to the number of classes of the dataset, we perform a 2-step incremental learning task on PACS and both 5-step and 10-step incremental tasks on OfficeHome and DomainNet, similar to Simon et al. (2022).

Evaluation Metric. Domain-wise average accuracy is normally used for domain generalization tasks to evaluate the generalization capability of the model (Gulrajani and Lopez-Paz, 2021). Under DGCIL conditions, we also need to evaluate the memorizing capability of the model and consider performance on old and new classes, respectively. Thus, during each learning session, we first regard one domain as the unseen domain and the remaining domains as training domains to train the model. Then the domain-wise class-wise average accuracy is reported as the overall performance of the model. We also use the domain-wise harmonic accuracy between old and new classes to evaluate for possible prediction bias. Each domain becomes a test domain at once, e.g., given four domains we have four separate sets of experiments to average over. Moreover, our evaluation protocol is explained in Figure 4 (left). We argue that the protocol of MSL_MOV (right) may be biased to overestimate the performance on old classes. This may occur due to accuracy being averaged over sub-tasks, or it might even result in an overestimation of overall accuracy if early sub-tasks align more closely with the test domain than the whole task. To address this concern, we propose evaluating all models at the end of each incremental session.

Model Selection. As the model selection is non-trivial for domain generalization, following domain generalization benchmark DomainBed (Gulrajani and Lopez-Paz, 2021), we use the training-domain validation set strategy to select the final model for all the experiments. Specifically, we split each training domain into 80% and 20% for training and validation subsets, respectively. We combine the validation subsets from all training domains to generate the overall validation set. The model that provides the maximal domain-wise class-wise accuracy on the overall validation set is chosen as the final model.

Table 1: Domain-wise average performance for each unseen domain over all incremental steps on the PACS dataset under the 2-step incremental setting.

Methods	PACS			
	2-Step Inc (+ 2 cls/step)			
	Art	Cartoon	Photo	Sketch
	average accuracy (% \uparrow)			
ERM	51.01	50.22	54.35	48.85
MixStyle (Zhou et al., 2021)	44.68	47.05	49.15	47.06
CORAL (Sun and Saenko, 2016)	50.32	51.26	54.50	50.20
EWC (Kirkpatrick et al., 2017)	52.01	50.03	54.57	50.25
MAS (Aljundi et al., 2018)	54.52	53.00	58.48	51.35
MSL_MOV (Simon et al., 2022)	56.76	52.55	56.79	48.96
MSL_MOV + Norm	54.40	53.45	60.76	51.92
MSL_MOV + Data Aug	57.56	55.99	70.22	53.99
MSL_MOV + Norm + Data Aug	64.11	49.59	70.84	63.20
MSL_MOV + Old Prototype	57.18	53.24	57.81	49.01
LwF (Li and Hoiem, 2017)	51.71	50.11	54.43	47.52
LwF + Norm (Li and Hoiem, 2017)	63.91	64.79	68.67	59.80
LwF + Norm + Data Aug	69.43	72.62	76.63	55.60
TRIPS (ours) + Data Aug	80.79	74.80	83.77	77.27
	harmonic accuracy (% \uparrow)			
ERM	0.0	0.0	0.0	0.0
MixStyle (Zhou et al., 2021)	0.0	0.0	0.0	0.0
CORAL (Sun and Saenko, 2016)	0.0	0.0	0.0	0.0
EWC (Kirkpatrick et al., 2017)	0.51	0.12	1.10	0.0
MAS (Aljundi et al., 2018)	11.71	10.81	15.84	5.13
MSL_MOV (Simon et al., 2022)	19.90	8.76	10.29	0.55
MSL_MOV + Norm	32.71	40.28	42.11	38.61
MSL_MOV + Data Aug	22.11	26.90	49.21	12.39
MSL_MOV + Norm + Data Aug	41.19	40.30	30.19	40.96
MSL_MOV + Old Prototype	19.82	9.12	11.07	1.01
LwF (Li and Hoiem, 2017)	0.0	0.11	0.05	0.0
LwF + Norm (Li and Hoiem, 2017)	47.33	50.60	52.06	42.11
LwF + Norm + Data Aug	59.02	66.85	66.52	24.35
TRIPS (ours) + Data Aug	74.16	68.04	73.58	70.47

Implementation Details. We build our code on top of domain generalization benchmark DomainBed (Gulrajani and Lopez-Paz, 2021). For our experiments, we use ResNet-34 (He et al., 2016) as the backbone network. The initial learning rate is set to 5e-5 for all dataset training. The maximum iteration is set to 5000 and we utilize the training-domain validation set strategy (Gulrajani and Lopez-Paz, 2021) to select the final model. We use a batch size of 32 for each training domain data and the final data for each batch training is the cascaded data from all training domains. To capture the possible performance variations due to data split and report accurate performance, we run each experiment on three seeds and report the average result.

5.1 Comparison with the State of the Art

We compare our method with exemplar-free incremental learning methods LwF (Li and Hoiem, 2017), EWC (Kirkpatrick et al., 2017), and MAS (Aljundi et al., 2018). We also compare our method with domain generalization methods CORAL (Sun and Saenko, 2016) and MixStyle (Zhou et al., 2021), and DGCIL method MSL_MOV (Simon et al., 2022). Experiments are performed on three datasets (Li et al., 2017; Venkateswara et al., 2017; Saito et al., 2019) under several different incremental settings. DGCIL is a challenging task that combines the difficulty of both incremental learning and domain generalization. To comprehensively evaluate the performance of each method, its memorizing and generalization ca-

pabilities should be evaluated. Thus, we report the average performance towards all incremental steps for each domain to evaluate the out-of-distribution performance. We also report the average performance towards all domains for each incremental step to evaluate the preservation of past knowledge.

Figure 5 and Table 1 show the experimental results on the PACS dataset. During experiments, we find that applying batch normalization on the features from the feature extractor is important to boost performance. We conjecture this is because, during training, there are covariate shifts (Ioffe and Szegedy, 2015), and the shifting is more severe when the training data comes from various domains. To make fair comparisons, we apply the same batch normalization to all distillation-based methods. In addition, for small dataset training, data augmentation is important to guarantee sufficient data is available for training. Thus, we apply image rotations by 90 degrees on the training data and regard the rotated images as additional classes to increase both the number of samples and class concepts. In each incremental step, we apply this data and class augmentation strategy in our method when the number of new classes is below 5. For fair comparisons, we apply the same augmentation strategy to our method and other methods.

We also note that MSL_MOV is an exemplar-based method by design. However, we study the exemplar-free setting in this paper. Thus, for a fair comparison, we equip MSL_MOV with mean-based prototypes and we completely remove exemplars from MSL_MOV⁴.

According to Table 1, TRIPS always achieves the best performance on different unseen test domains. We have an average of 8.69% and 12.94% gain on average and harmonic accuracy compared to the second-best method, respectively. When the hardest *sketch* domain is the unseen test domain, our method outperforms SOTA by 14.07% and 28.36% in average and harmonic accuracy, respectively. This shows TRIPS copes well with such an out-of-distribution scenario. Figure 5 shows that TRIPS also achieves both the highest average accuracy and harmonic accuracy for all the incremental steps.

Figure 6 and Table 2 show the experimental results on OfficeHome and DomainNet datasets. Under both five-step and ten-step incremental settings, TRIPS shows significant improvements over the baselines. According to Table 2, under four different task settings, we outperform the second-best baseline by an average of 13.78%/15.86% on average/harmonic accuracy for all domains which shows our method copes well with the out-of-distribution test data. According to Figure 6, under four different task settings, we also outperform the second-best baseline in almost every step on both average and harmonic accuracy which shows our method is more robust to catastrophic forgetting.

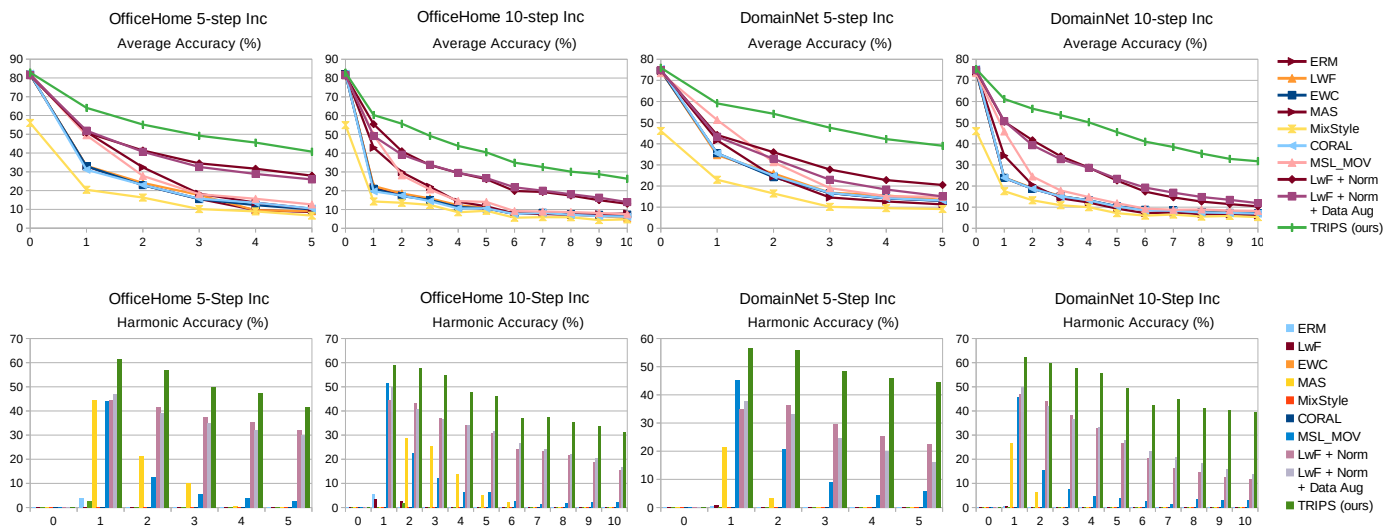
5.2 Ablation Study

To validate the effectiveness of each part of our method, Tables 3 and A.5 show the ablation study on the OfficeHome

⁴Prototype-based IL methods usually perform worse than exemplar-based IL methods. Thus, the performance of MSL_MOV reported by Simon et al. (2022) differs from the performance reported in our paper due to (i) prototype-based “memory” and a more realistic evaluation setting as in Figure 4 (left).

Table 2: Domain-wise average performance over all incremental steps on OfficeHome and DomainNet under *the 5-step and 10-step incremental settings*.

Methods	OfficeHome								DomainNet							
	5-Step Inc (+ 10 cls/step)				10-Step Inc (+ 5 cls/step)				5-Step Inc (+ 20 cls/step)				10-Step Inc (+ 10 cls/step)			
	Art	Clipart	Product	Real	Art	Clipart	Product	Real	Clipart	Painting	Real	Sketch	Clipart	Painting	Real	Sketch
	average accuracy (% \uparrow)															
ERM	26.55	26.85	31.95	32.41	16.19	16.19	18.81	19.49	30.60	27.69	30.64	30.09	18.11	16.59	18.04	17.79
MixStyle (Zhou et al., 2021)	15.16	18.96	22.33	21.87	10.15	12.27	14.04	14.32	21.12	16.85	17.98	20.64	13.21	10.44	11.79	13.27
CORAL (Sun and Saenko, 2016)	27.39	26.91	31.52	32.34	16.12	15.79	18.31	19.11	30.32	28.45	31.05	30.06	18.12	16.77	18.15	17.87
EWC (Kirkpatrick et al., 2017)	26.85	27.00	32.60	31.71	16.07	16.94	18.53	19.34	30.45	27.95	30.45	30.01	18.11	16.57	18.24	17.94
MAS (Aljundi et al., 2018)	29.95	30.56	41.83	36.51	19.32	21.28	22.51	24.01	29.86	28.26	31.86	30.22	18.14	16.37	19.74	17.99
MSL_MOV (Simon et al., 2022)	30.43	30.65	36.62	39.29	19.68	20.81	23.81	27.05	33.52	31.69	37.87	33.64	20.66	19.59	23.00	21.08
LwF (Li and Hoiem, 2017)	26.82	26.95	32.15	33.02	16.07	16.81	19.21	20.59	30.60	28.05	29.89	30.08	17.91	15.88	18.64	17.82
LwF + Norm	38.06	41.17	47.77	51.46	25.83	28.37	34.45	39.21	36.25	34.62	40.41	39.32	29.10	26.81	30.84	29.06
LwF+Norm+Data Aug	40.03	37.92	46.98	49.02	30.85	27.66	33.59	34.98	35.92	31.59	35.20	35.60	31.62	26.02	31.10	29.78
TRIPS (ours)	46.04	48.99	62.24	67.88	33.87	38.64	49.57	54.39	54.20	47.36	55.35	55.22	47.80	42.41	50.37	49.41
	harmonic accuracy (% \uparrow)															
ERM	0.63	0.84	0.14	0.0	0.10	0.33	0.48	1.25	0.15	0.08	0.03	0.08	0.09	0.10	0.01	0.04
MixStyle (Zhou et al., 2021)	0.0	0.01	0.0	0.0	0.0	0.0	0.04	0.0	0.01	0.0	0.02	0.0	0.0	0.0	0.02	0.0
CORAL (Sun and Saenko, 2016)	0.0	0.0	0.02	0.01	0.0	0.0	0.1	0.2	0.0	0.0	0.01	0.0	0.0	0.05	0.01	0.01
EWC (Kirkpatrick et al., 2017)	0.24	0.13	2.32	0.03	0.09	0.54	0.0	0.02	0.20	0.02	0.30	0.0	0.06	0.11	0.12	0.11
MAS (Aljundi et al., 2018)	5.60	16.85	20.08	10.65	7.03	12.17	7.68	7.26	4.59	4.20	5.15	2.89	3.32	2.15	4.69	3.10
MSL_MOV (Simon et al., 2022)	10.69	11.41	14.75	18.23	7.47	9.70	11.40	15.28	13.31	12.58	18.20	12.68	8.42	8.13	11.20	8.85
LwF (Li and Hoiem, 2017)	0.23	0.46	0.0	0.0	0.10	0.08	0.16	0.25	0.15	0.10	0.25	0.12	0.09	0.12	0.03	0.01
LwF + Norm	31.14	37.02	40.49	44.36	20.84	26.88	32.35	37.04	22.71	22.30	28.30	25.58	26.62	24.20	29.36	25.83
LwF+Norm+Data Aug	34.00	31.87	39.05	41.63	29.72	26.19	31.77	33.75	22.68	19.71	22.88	22.77	30.05	24.20	29.98	28.19
TRIPS (ours)	39.56	44.89	57.46	63.71	32.40	39.07	49.68	55.10	42.88	36.97	44.50	43.28	49.93	44.49	52.45	50.59

Fig. 6: Domain-average performance of each incremental step under *the 5-step and 10-step incremental settings* on the OfficeHome and DomainNet datasets.

dataset (Venkateswara et al., 2017). Firstly, when the triplet loss is used (which improves the generalization of the model), in the base step, the average accuracy of the model improves by 1.60%. During incremental learning, the triplet loss improves the average/harmonic accuracy in each incremental step for every test domain by an average of 12.06%/11.34%. Thus, the benefit of triplet loss is clear. Next, we update and inject old-class prototypes into both the cross-entropy and triplet loss. We find that directly injecting updated old-class prototypes does not help improve the performance. We conjecture this is because of the extreme data imbalance since we focus on the exemplar-free setting and each old class only has one mean-based prototype preserved. Thus, to overcome the data imbalance and obtain balanced old- and new-class performance,

sufficient pseudo-features of old classes are sampled from the updated class prototype representations. With the help of sampling, the performance is boosted by an average of 1.57%/1.47% average/harmonic accuracy over all incremental steps.

5.3 Comparison of Different Prototype Representations

To validate the efficiency of our proposed prototype representation based on the multivariate Normal distribution (mean and covariance matrix per class) and our pseudo-sampling strategy, we compare our method with related prototype representation methods (Yu et al., 2020; Zhu et al., 2021a). SDC (Yu et al., 2020) utilizes the single mean-based prototype per class and a non-parametric cosine classifier. SDC updates old-class means by shifting them through the lens of new-class samples and uses

Table 3: Ablations on OfficeHome under *the five-step incremental setting* (ten new classes added at a time). Results use format $a(b, c, d, e)$ where a is (top) the average and (bottom) harmonic accuracy over all four test domains, whereas (b, c, d, e) represents (top) the average and (bottom) harmonic accuracy per test domain: art, clipart, product, real. The detailed performance for steps 3, 4, and 5 are reported in the supplementary material due to space limitations.

KD	triplet	proto shift	pseudo sampling	0 (base)		1				2				3		4		5	
				Domain-Average (Art, Clipart, Product, Real)															
average accuracy (% ↑)																			
✓				81.29 (76.26 70.83 86.82 91.27)	50.89 (44.71 47.99 54.12 56.73)	41.37 (33.12 38.64 46.38 47.35)	34.52	31.67	27.94										
✓	✓			82.89 (79.33 72.20 87.74 92.30)	60.85 (49.97 56.35 66.60 70.48)	52.97 (39.22 47.42 60.48 64.74)	47.62	44.81	40.18										
✓	✓	✓		82.89 (79.33 72.20 87.74 92.30)	60.73 (49.39 53.84 69.50 70.19)	53.38 (40.61 46.17 61.50 65.26)	48.27	44.68	39.92										
✓	✓	✓	✓	82.89 (79.33 72.20 87.74 92.30)	64.08 (50.21 58.33 71.45 76.31)	55.18 (42.83 48.25 62.23 67.42)	49.25	45.58	40.74										
harmonic accuracy (% ↑)																			
✓				-	44.45 (40.32 45.81 44.98 46.71)	41.58 (32.74 39.43 46.25 47.89)	37.49	35.52	32.22										
✓	✓			-	58.06 (43.55 55.76 63.33 69.61)	54.35 (38.03 49.71 62.42 67.24)	48.83	46.42	40.30										
✓	✓	✓		-	58.09 (42.81 52.07 68.16 69.30)	55.51 (41.78 48.17 64.13 67.93)	49.63	46.50	39.95										
✓	✓	✓	✓	-	61.45 (43.17 57.30 69.15 76.16)	57.11 (44.33 50.42 63.94 69.74)	49.76	47.22	41.51										

Table 4: Comparison of our sampling strategy with other pseudo-sampling methods, *i.e.*, SDC (Yu et al., 2020) and PASS (Zhu et al., 2021a) under *the five-step incremental setting* (10 new classes added at a time) on the OfficeHome dataset.

	0 (base)		1					2					3					4					5				
	average accuracy (% ↑)																										
MSL_MOV	81.80	49.49	27.84	18.08	15.65	12.62																					
MSL_MOV with SDC	81.80	50.31	28.62	19.01	16.04	13.08																					
TRIPS w/o prototypes	82.89	60.85	52.97	47.62	44.81	40.18																					
TRIPS with SDC	82.89	60.73	53.38	48.27	44.68	39.92																					
TRIPS with PASS	82.89	63.37	53.53	48.08	43.92	39.07																					
TRIPS (ours)	82.89	64.08	55.18	49.25	45.58	40.74																					
harmonic accuracy (% ↑)																											
MSL_MOV	-	44.16	12.70	5.39	3.79	2.80																					
MSL_MOV with SDC	-	44.21	13.02	6.07	4.13	3.05																					
TRIPS w/o prototypes	-	58.06	54.35	48.83	46.42	40.30																					
TRIPS with SDC	-	58.09	55.51	49.63	46.50	39.95																					
TRIPS with PASS	-	59.51	55.20	49.11	46.51	40.82																					
TRIPS (ours)	-	61.45	57.11	49.76	47.22	41.51																					

updated class-wise means for classification. As in SDC, the final classification result is determined by the maximum cosine similarity over the feature vector of an input image and the updated class-wise mean-based prototypes. SDC does not sample pseudo-features of old classes as it is impossible to perform sampling from first-order statistics such as the mean.

PASS (Zhu et al., 2021a) uses the mean-based prototype with a radius (hyper-parameter) to form an isotropic Normal distribution from which pseudo-features of old classes are sampled. The formula $\phi'_c = \mu'_c + \gamma \mathbf{v}$ describes the sampling step, where ϕ'_c are the sampled pseudo-features of old class c at session t and μ'_c is the mean-based prototype for old class c at session t . Moreover, $\mathbf{v} \sim \mathcal{N}(\mathbf{0}, \mathbb{I})$ is a vector sampled from the isotropic Normal distribution, whereas $\gamma \geq 0$ is the radius that controls the deviation of pseudo-features from the mean.

We implement the SDC and PASS methods in our setting using their official code available online. As MSL_MOV is an exemplar-based method which does not utilize old-class prototypes, for a fair comparison, we implement it with SDC (updated old prototypes).

Table 4 shows that modeling prototype representations as full multivariate Normal distributions per class outperforms the naive use of isotropic Normal distributions with distinct means per class.

5.4 Hyper-parameter Analysis

To find the most suitable hyper-parameter value, we perform the hyper-parameter grid analysis on the PACS dataset under the two-step incremental protocol. Figure 8 shows the analysis for different loss terms. To better explore the effect of each loss term, these experiments are trained without data augmentation and pseudo-sampling. Five old exemplars for each class and each domain are stored and utilized. Firstly, we set the distillation loss term hyper-parameter (λ') to 1 and vary the value for the triplet loss term hyper-parameter (λ). We find that when λ is set to 1, the best average and harmonic accuracy are acquired. Then we set λ to 1 and vary the value for λ' . We find that when λ' is set to 30, the best average and harmonic accuracy are acquired. Thus, for all our experiments, we set λ to 1 and λ' to 30. We do a similar loss term hyper-parameter grid search for other methods. For all distillation-based methods (Li and Hoiem, 2017; Simon et al., 2022) we use the hyper-parameter value 30 for the distillation loss. For importance matrix-based methods (Kirkpatrick et al., 2017; Aljundi et al., 2018), we use the hyper-parameter value 1000 for the regularization loss.

We also explore the effect of various hyper-parameters related to prototype shifting and pseudo-sampling. Figure 7 shows the values of hyper-parameters we set for shifting factor (σ), moving average factor (η), and shrinkage factor (α). Firstly, we set $\eta = 0.1$ and $\alpha = 0.1$, and vary the value of σ . When σ is set to 0.5, the best performance is obtained. Then, we set $\sigma = 0.5$ and $\alpha = 0.1$, and vary the value of η . When η is set to 0.1, the best performance is obtained. After that, we set $\sigma = 0.5$ and $\eta = 0.1$, and vary the value of α . When α is set to 0.05, the best performance is obtained. These parameters were selected on the PACS dataset and then simply applied without any tuning on both OfficeHome and DomainNet datasets. We also observed that the same hyper-parameters were optimal when we used the validation set of PACS comprised of the three training domains of PACS and 20% train data withheld for validation.

5.5 Backbone Analysis

To validate that the benefits of the proposed method are independent of the used backbone network, we perform experiments based on other backbones instead of ResNet-34. Figures 9 and

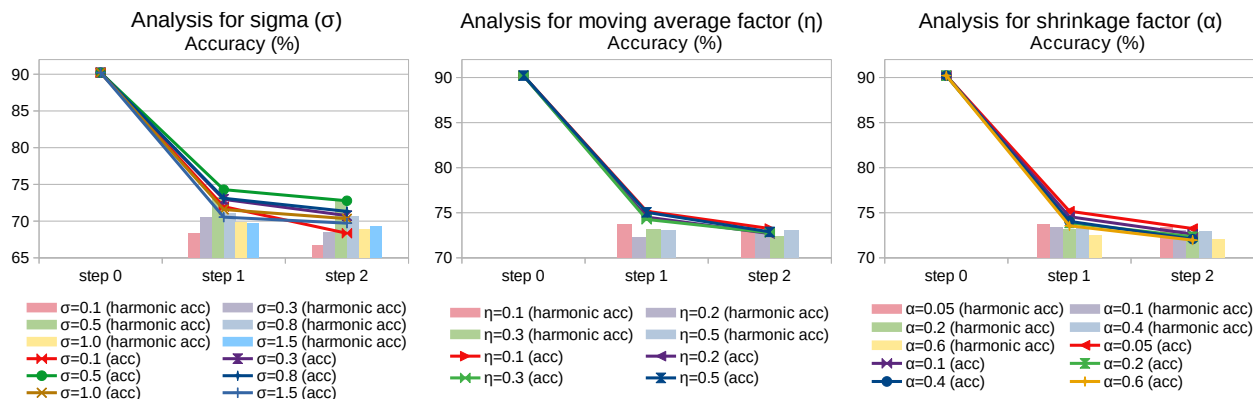


Fig. 7: Ablations of prototype shifting and pseudo-sampling hyper-parameters σ , η , and α on the PACS dataset.

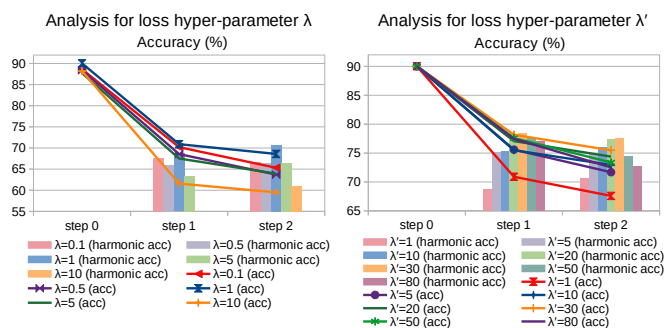


Fig. 8: Ablations of loss hyper-parameters λ and λ' on the PACS dataset.

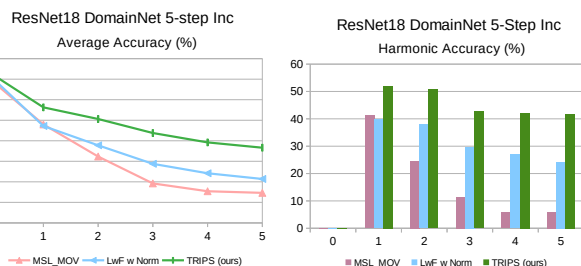


Fig. 10: Performance under *the five-step incremental settings* (20 new classes added at a time) on the DomainNet dataset based on ResNet-18.

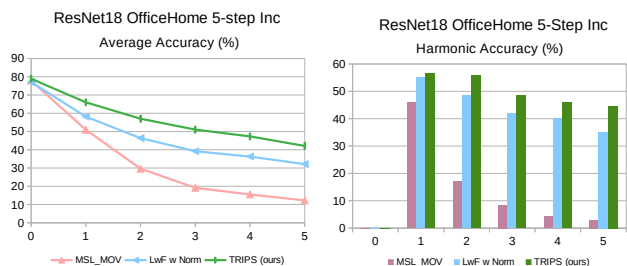


Fig. 9: Performance under *the five-step incremental settings* (10 new classes added at a time) on the OfficeHome dataset based on ResNet-18.

10 show the comparison with other methods on the OfficeHome (Venkateswara et al., 2017) and DomainNet (Saito et al., 2019) datasets using ResNet-18 as the backbone network. In both settings, our TRIPS method always achieves the best performance.

5.6 Training Time Analysis

We run all our experiments on 1x NVIDIA v100 GPU with 16GB RAM. We use a batch size of 32 for each domain set, and three training domains are utilized in each batch. Thus, the total batch size is 96. When data augmentation is utilized, due to memory limitations, we reduce the batch size from 32 to 24 for each domain set, thus the total batch size is reduced from 96 to 72. For each incremental session, the training time is between 5 and 7 hours. When data augmentation is utilized, the training data within each batch is enlarged from 72 to 288,

which causes the training time to increase to be between 10 and 15 hours long per incremental session. Within each batch, an equal number of pseudo-samples from old classes will be generated from the multivariate Normal distributions (this step do not rely on a feature extractor minimizing the impact on run-time). These samples of old classes are used along the samples from the new classes.

6 Conclusions

In this paper, we have explored the challenging DGCIL task and proposed our TRIPS method. To improve the generalization of the model, triplet loss helps obtain semantic information while eliminating domain information. With no old exemplars preserved, we sample pseudo-features of old classes from updated prototype representations (multivariate Normal distributions). These pseudo-features not only help preserve old class knowledge but also support the TRIPS loss to maintain inter-class boundaries, thus boosting the performance. Importantly, these prototype representations are domain-agnostic as our loss enforces domain confusion. Substantial improvements in benchmarks demonstrate the efficiency of our method.

Acknowledgements

This work was funded by CSIRO's Reinvent Science and CSIRO's Data61 Science Digital.

References

- Aljundi, R., Babiloni, F., Elhoseiny, M., Rohrbach, M., Tuytelaars, T., 2018. Memory aware synapses: Learning what (not) to forget, in: *European Conference on Computer Vision*, pp. 139–154.
- Arjovsky, M., Bottou, L., Gulrajani, I., Lopez-Paz, D., 2019. Invariant risk minimization. *arXiv preprint arXiv:1907.02893*.
- Buzzega, P., Boschini, M., Porrello, A., Abati, D., Calderara, S., 2020. Dark experience for general continual learning: a strong, simple baseline. *Advances in neural information processing systems* 33, 15920–15930.
- Chaudhry, A., Dokania, P.K., Ajanthan, T., Torr, P.H., 2018. Riemannian walk for incremental learning: Understanding forgetting and intransigence, in: *European Conference on Computer Vision*, pp. 532–547.
- Dou, Q., Coelho de Castro, D., Kamnitsas, K., Glocker, B., 2019. Domain generalization via model-agnostic learning of semantic features. *Advances in Neural Information Processing Systems* 32.
- Douillard, A., Ramé, A., Couairon, G., Cord, M., 2022. Dytox: Transformers for continual learning with dynamic token expansion, in: *Proceedings of the IEEE/CVF Conference on Computer Vision and Pattern Recognition*, pp. 9285–9295.
- Gulrajani, I., Lopez-Paz, D., 2021. In search of lost domain generalization, in: *International Conference on Learning Representations*.
- He, K., Zhang, X., Ren, S., Sun, J., 2016. Deep residual learning for image recognition, in: *Proceedings of the IEEE conference on computer vision and pattern recognition*, pp. 770–778.
- Hinton, G., Vinyals, O., Dean, J., et al., 2015. Distilling the knowledge in a neural network. *arXiv preprint arXiv:1503.02531* 2.
- Hou, S., Pan, X., Loy, C.C., Wang, Z., Lin, D., 2019. Learning a unified classifier incrementally via rebalancing, in: *Proceedings of the IEEE/CVF Conference on Computer Vision and Pattern Recognition*, pp. 831–839.
- Ioffe, S., Szegedy, C., 2015. Batch normalization: Accelerating deep network training by reducing internal covariate shift, in: *International conference on machine learning*, pmlr. pp. 448–456.
- Ji, Z., Li, J., Wang, Q., Zhang, Z., 2022. Complementary calibration: Boosting general continual learning with collaborative distillation and self-supervision. *IEEE Transactions on Image Processing*.
- Kirkpatrick, J., Pascanu, R., Rabinowitz, N., Veness, J., Desjardins, G., Rusu, A.A., Milan, K., Quan, J., Ramalho, T., Grabska-Barwinska, A., et al., 2017. Overcoming catastrophic forgetting in neural networks. *Proceedings of the national academy of sciences* 114, 3521–3526.
- Knights, J., Moghadam, P., Ramezani, M., Sridharan, S., Fookes, C., 2022. Incloud: Incremental learning for point cloud place recognition, in: *2022 IEEE/RSJ International Conference on Intelligent Robots and Systems (IROS)*, IEEE. pp. 8559–8566.
- Krueger, D., Caballero, E., Jacobsen, J.H., Zhang, A., Binas, J., Zhang, D., Le Priol, R., Courville, A., 2021. Out-of-distribution generalization via risk extrapolation (rex), in: *International Conference on Machine Learning*, PMLR. pp. 5815–5826.
- Ledoit, O., Wolf, M., 2004. Honey, i shrunk the sample covariance matrix. *The Journal of Portfolio Management* 30, 110–119.
- Li, D., Yang, Y., Song, Y.Z., Hospedales, T.M., 2017. Deeper, broader and artier domain generalization, in: *International Conference on Computer Vision*, pp. 5542–5550.
- Li, J., Ji, Z., Wang, G., Wang, Q., Gao, F., 2022. Learning from students: Online contrastive distillation network for general continual learning, in: *Proc. 31st Int. Joint Conf. Artif. Intell.*, pp. 3215–3221.
- Li, Z., Hoiem, D., 2017. Learning without forgetting. *IEEE transactions on pattern analysis and machine intelligence* 40, 2935–2947.
- Liu, Z., Milano, F., Frey, J., Siegwart, R., Blum, H., Cadena, C., 2023. Unsupervised continual semantic adaptation through neural rendering, in: *Proceedings of the IEEE/CVF Conference on Computer Vision and Pattern Recognition*, pp. 3031–3040.
- Rebuffi, S.A., Kolesnikov, A., Sperl, G., Lampert, C.H., 2017. icarl: Incremental classifier and representation learning, in: *Proceedings of the IEEE conference on Computer Vision and Pattern Recognition*, pp. 2001–2010.
- Roy, K., Simon, C., Moghadam, P., Harandi, M., 2023. Subspace distillation for continual learning. *Neural Networks* 167, 65–79.
- Saito, K., Kim, D., Sclaroff, S., Darrell, T., Saenko, K., 2019. Semi-supervised domain adaptation via minimax entropy, in: *International Conference on Computer Vision*, pp. 8050–8058.
- Simon, C., Faraki, M., Tsai, Y.H., Yu, X., Schuler, S., Suh, Y., Harandi, M., Chandraker, M., 2022. On generalizing beyond domains in cross-domain continual learning, in: *Proceedings of the IEEE/CVF Conference on Computer Vision and Pattern Recognition*, pp. 9265–9274.
- Simon, C., Koniusz, P., Harandi, M., 2021. On Learning the Geodesic Path for Incremental Learning, in: *Proceedings of the IEEE/CVF Conference on Computer Vision and Pattern Recognition*.
- Sun, B., Saenko, K., 2016. Deep coral: Correlation alignment for deep domain adaptation, in: *European conference on computer vision*, Springer. pp. 443–450.
- Venkateswara, H., Eusebio, J., Chakraborty, S., Panchanathan, S., 2017. Deep hashing network for unsupervised domain adaptation, in: *Proceedings of the IEEE/CVF Conference on Computer Vision and Pattern Recognition*, pp. 5018–5027.
- Volpi, R., Larlus, D., Rogez, G., 2021. Continual adaptation of visual representations via domain randomization and meta-learning, in: *Proceedings of the IEEE/CVF Conference on Computer Vision and Pattern Recognition*, pp. 4443–4453.
- Xie, J., Yan, S., He, X., 2022. General incremental learning with domain-aware categorical representations, in: *Proceedings of the IEEE/CVF Conference on Computer Vision and Pattern Recognition*, pp. 14351–14360.
- Yoon, J., Yang, E., Lee, J., Hwang, S.J., 2018. Lifelong learning with dynamically expandable networks, in: *International Conference on Learning Representations*.
- Yu, L., Twardowski, B., Liu, X., Herranz, L., Wang, K., Cheng, Y., Jui, S., Weijer, J.v.d., 2020. Semantic drift compensation for class-incremental learning, in: *Proceedings of the IEEE/CVF Conference on Computer Vision and Pattern Recognition*, pp. 6982–6991.
- Zhang, H., Cisse, M., Dauphin, Y.N., Lopez-Paz, D., 2018. mixup: Beyond empirical risk minimization, in: *International Conference on Learning Representations*.
- Zhou, K., Yang, Y., Qiao, Y., Xiang, T., 2021. Domain generalization with mixstyle, in: *International Conference on Learning Representations*.
- Zhu, F., Zhang, X.Y., Wang, C., Yin, F., Liu, C.L., 2021a. Prototype augmentation and self-supervision for incremental learning, in: *Proceedings of the IEEE/CVF Conference on Computer Vision and Pattern Recognition*, pp. 5871–5880.
- Zhu, K., Cao, Y., Zhai, W., Cheng, J., Zha, Z.J., 2021b. Self-promoted prototype refinement for few-shot class-incremental learning, in: *Proceedings of the IEEE/CVF Conference on Computer Vision and Pattern Recognition*, pp. 6801–6810.

Supplementary Material

Appendix A Ablation Study

To validate the effectiveness of each part of our method, we perform the ablation study on OfficeHome (Venkateswara et al., 2017). The experimental results are shown in Table 3 and A.5.

Firstly, to improve the generalization of the model, the triplet loss is applied to extract semantic information while suppressing domain information. Observing the experimental results, the benefit of triplet loss is clear. Then, we update old class prototypes and sample pseudo-old class features from the updated prototypes. With the help of the multivariate sampling strategy, the performance is further boosted.

Table A.5: Ablations on OfficeHome under *the 5-step incremental setting* (10 new classes added at a time). Results use format $a(b, c, d, e)$ where a is (top) the average and (bottom) harmonic accuracy over all four test domains, whereas (b, c, d, e) represents (top) the average and (bottom) harmonic accuracy per test domain: art, clipart, product, real.

KD	triplet	proto shift	pseudo sampling	0 (base)	1	2	3	4	5
				Domain-Average (Art, Clipart, Product, Real)					
				average accuracy (% \uparrow)					
✓				81.29	50.89	41.37	34.52 (27.64, 32.96, 37.60, 39.88)	31.67 (24.97, 30.04, 33.36, 38.31)	27.94 (21.65, 26.54, 28.37, 35.21)
✓	✓			82.89	60.85	52.97	47.62 (36.95, 40.89, 53.56, 59.08)	44.81 (34.27, 37.98, 49.69, 57.32)	40.18 (31.32, 33.47, 44.71, 51.19)
✓	✓	✓		82.89	60.73	53.38	48.27 (37.01, 41.98, 55.20, 58.90)	44.68 (34.21, 38.42, 49.94, 56.14)	39.92 (30.58, 33.84, 44.38, 50.86)
✓	✓	✓	✓	82.89	64.08	55.18	49.25 (37.76, 42.74, 55.45, 61.03)	45.58 (34.71, 38.45, 51.06, 58.12)	40.74 (31.39, 33.97, 45.49, 52.13)
				harmonic accuracy (% \uparrow)					
✓				-	44.45	41.58	37.49 (30.07, 35.84, 40.84, 43.21)	35.52 (27.76, 33.57, 37.55, 43.19)	32.22 (24.81, 30.46, 32.83, 40.79)
✓	✓			-	58.06	54.35	48.83 (38.95, 42.26, 54.28, 59.84)	46.42 (37.18, 38.61, 50.81, 59.09)	40.30 (32.65, 32.96, 44.41, 51.16)
✓	✓	✓		-	58.09	55.51	49.63 (39.24, 42.90, 56.59 , 59.80)	46.50 (37.00, 38.92 , 51.58, 58.52)	39.95 (31.68, 33.96, 44.54, 49.63)
✓	✓	✓	✓	-	61.45	57.11	49.76 (39.26, 43.62, 55.96, 60.19)	47.22 (37.50, 38.58, 52.73, 60.06)	41.51 (33.56, 34.55, 45.54, 52.37)